

Section 3

DEVELOPMENTS IN MICROFABRICATION

3.A Inertial Fusion Target-Mounting Methods: New Fabrication Procedures Reduce the Mounting Support Perturbation

Inertial fusion targets require a high degree of geometrical perfection for optimum, fusion-implosion performance. Theoretical design considerations establish exacting specifications for target fuel-core sphericity, target layer-thickness uniformity, and target surface smoothness for calculated fuel compressions. Recent target fabrication activities have concentrated on developing processes capable of both producing and verifying these exacting specifications. This section reports on research aimed at minimizing the geometrical imperfection caused by the use of fusion target delivery supports.

Current laser-fusion target delivery systems use thin fibers or films to support and position the target at the focal volume of the irradiation system. Using current procedures (100- μm -diameter \times 1- μm -wall glass microballoon bonded on a 10- μm -diameter glass fiber, for example), the constituting support mass introduced into the implosion dynamics is often a substantial fraction of the total target mass—a significant contribution to target asymmetry. The critical requirements for target delivery have been examined with the goal of identifying and developing techniques which (1) minimize the adverse effects of the support on target performance through geometry and material selection, (2) have application to the range of targets currently of interest in the fusion program, (3) can be implemented without major modification of target chamber engineering, and (4) have an acceptably low rate of target delivery loss. Target injection or levitation system schemes do not meet these requirements.¹ We have developed two new target delivery sys-

tems, based on mechanical supports, that have reduced the effective target support mass by a factor of 1000 below usual values and that have produced demonstrated improvements in target implosion symmetry.

Target delivery supports influence implosion performance through (1) the asymmetry introduced by the support and (2) the material mismatch between the support and the outer target surface. These two considerations establish guidelines, listed below, for improving target delivery systems. For asymmetry, the effective support mass (the target support material that is within a distance ℓ of the target surface) can influence the implosion dynamics. For material mismatch, support material having an atomic number different from the material of the target surface can give rise to magnetic fields which can affect implosion dynamics.

Two representative target delivery support systems commonly used are the fiber and the film mount. The fiber support material has usually been a drawn glass capillary or short silica, carbon, boron, or polymer filament adhesively bonded to the target. The film material has usually been formvar. Figure 28 shows the relationship between the effective

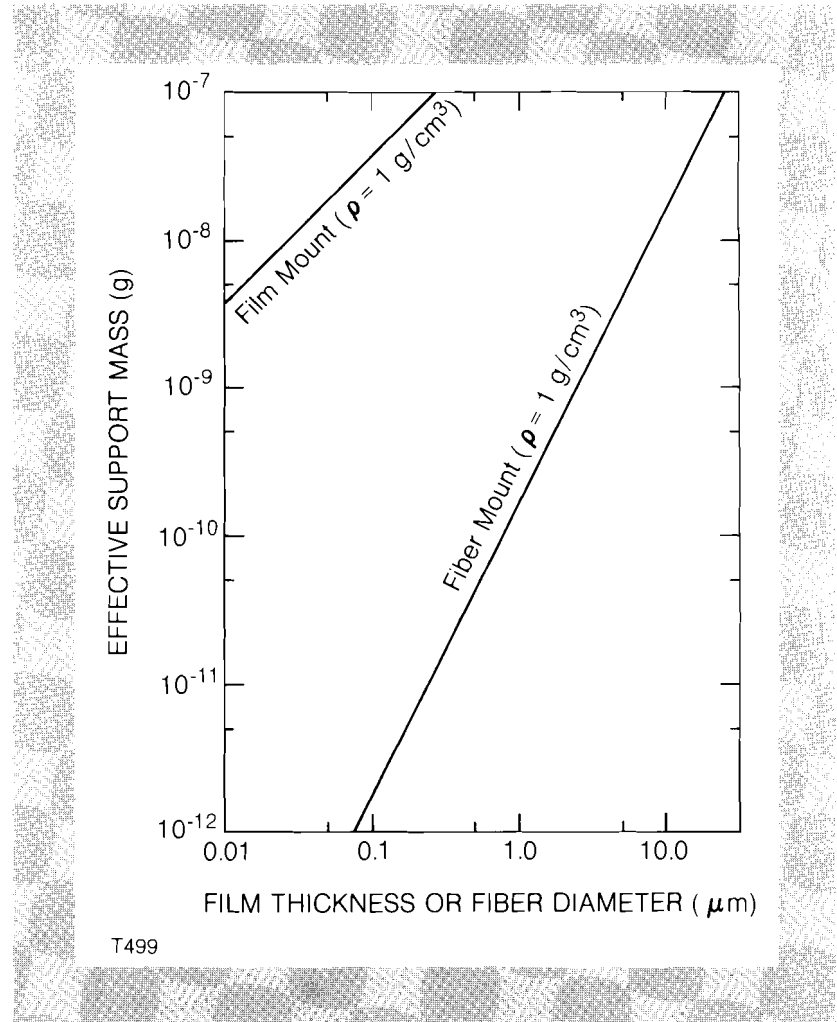


Fig. 28

Relationship between effective target-support mass and support dimension. The material densities of the film and the fiber are 1 g/cm^3 , the target diameter is $400 \text{ } \mu\text{m}$, and support influence range is $200 \text{ } \mu\text{m}$.

support mass introduced by each delivery system and the nominal support dimensions. Here d is the fiber diameter or the film thickness. These calculations are based on a 400- μm -diameter target, an assumed support influence range of $\ell = 200\ \mu\text{m}$, a support material density of $1\ \text{g}/\text{cm}^3$, and no added mass from adhesive material used to attach the target to the support. Nominal dimension values reported in the literature for these two target delivery systems are fiber diameters $\geq 10\ \mu\text{m}$ and film thicknesses $\geq 0.01\ \mu\text{m}$. As Fig. 28 demonstrates, comparable effective support masses result with a 100- \AA -thick formvar film ($\rho = 1\ \text{g}/\text{cm}^3$) and a 3.5- μm -diameter glass fiber ($\rho = 2.5\ \text{g}/\text{cm}^3$). For reference in this figure, a 100- μm -diameter \times 1- μm -wall glass balloon has a mass of $8 \times 10^{-8}\ \text{g}$.

The slope of the fiber support curve in Fig. 28 is larger than that of the film support curve, indicating that greater reduction in target delivery support mass is achievable through reducing fiber rather than film dimensions. Target delivery systems based on film supports were not pursued for this technical reason. The next two sections describe procedures developed to fabricate and use micrometer and submicrometer diameter fibers to support and position fusion targets for irradiation experiments. Reported delivery reliability results are based on successfully positioning the target in the laser focal volume, evacuating the target chamber, and irradiating the target.

Two approaches were investigated for fabricating glass-fiber target supports. The first involved mounting the target on commercially available glass-fiber material using standard techniques.² Single fibers from Johns-Manville Tempstran glass wool³ having diameters in the range of 0.3 to 5 μm and lengths of approximately 1 cm were removed with forceps. One end of a fiber was bonded to a drawn glass capillary using UV curing epoxy. The free end was then either butt-mounted or tangentially mounted to the target surface using the same adhesive. Selecting, extracting, and handling individual fibers, performed with a stereo-microscope in previous target assemblies, proved difficult because of limited optical resolution. Practical handling considerations placed a lower limit of 2- μm diameter for this approach. Delivery reliability for $\leq 4\text{-}\mu\text{m}$ -diameter butt mounts was unacceptably low, but nearly 100% for tangential mounts made with 2- to 4- μm -diameter fibers. Another advantage, in addition to size, of these tangential fiber mounts over conventional drawn capillary butt mounts is the uniform cross-section of the fibers. Drawn capillaries with a 10- μm -diameter tip typically have a 3° taper, causing a 20- μm diameter at the 200- μm distance and giving a correspondingly effective mass increase.

The second glass-fiber target delivery system involved adhesively bonding a target to a fiber formed by performing additional drawing steps on conventional glass capillaries. This method, adapted from a technique developed by E. Diacumakos,⁴ circumvents the previously described fiber-handling difficulties. In brief, 1.5-mm-diameter glass capillary tubing is pulled to a tapered point using a micropipette puller. Viewing the operation through a 320-power, long-working-distance compound microscope, the point is pressed into a heated 0.25-mm-diameter Nichrome wire to form a molten glass bead $\sim 0.1\ \text{mm}$ in size.

With the wire still heated, the capillary tube is retracted 5 mm at a rate of 1 mm/s, causing glass material to be drawn from the molten bead to form a thin, constant-cross-section glass fiber. Current to the wire is then turned off. Further retraction of the capillary tube fractures the thin fiber, usually at the surface of the glass bead. This fiber fabrication process reproducibly forms fibers in the range of 0.75 to 1.5 μm in diameter.

Adhesively butt-mounting the produced fibers is difficult because of the small contact area present at the fiber tip, but reliable tangential mounts have been formed. However, a procedure for forming a 90° bend at the tip of the thin fiber has been developed; the bend provides increased adhesive contact area that allows formation of a reliable butt mount. This procedure involves pressing the thin glass fiber into the room temperature wire until noticeable deflection is evident near the tip. Current is applied to the wire to raise the fiber temperature to the glass softening point, causing a 90° bend to form near the fiber end. The bent section is usually 20 to 50 μm in length. Laser trimming of the fiber to a 10- μm length follows. Fiber attachment to the wire usually does not occur if the wire temperature is kept at a minimum. Figure 29 is a micrograph of a 400- μm -diameter target supported on a 0.8- μm -diameter bent fiber.

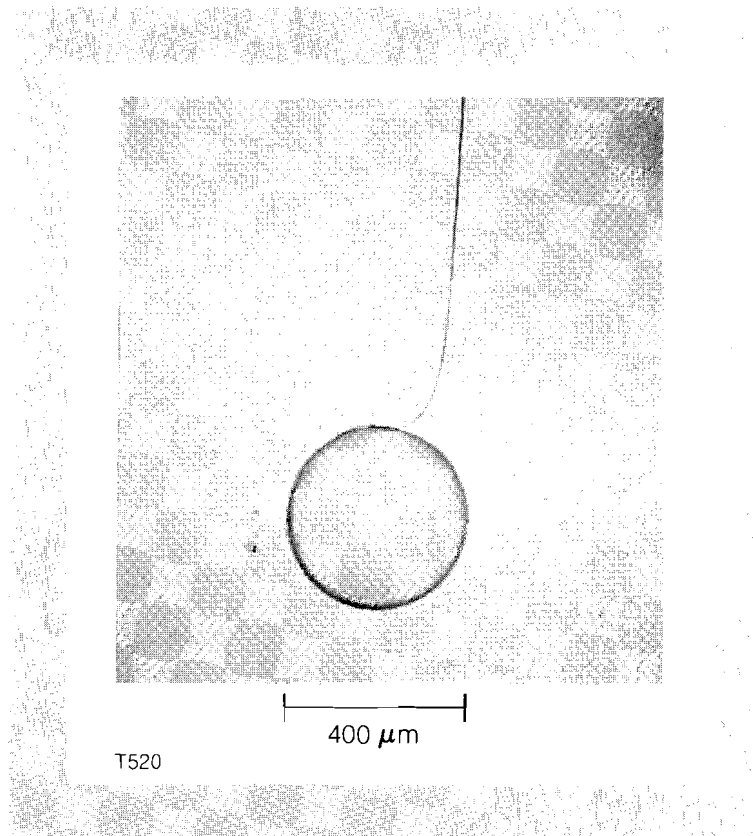
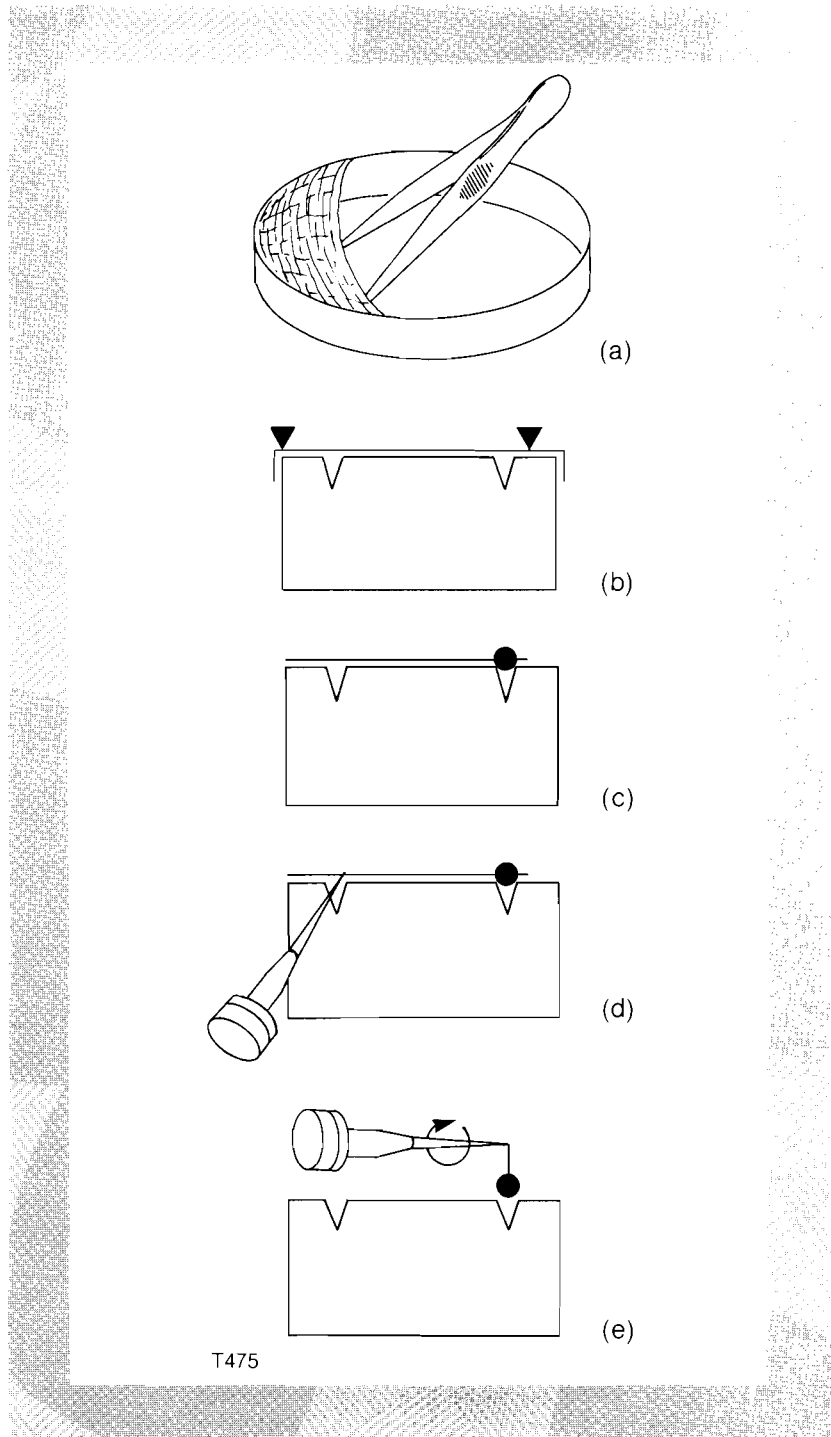


Fig. 29
SEM micrograph of fusion target supported with a drawn glass fiber.

Special efforts were required to apply correspondingly small quantities of adhesive on the thin glass fibers. Dow Corning Z-6040 silane coupling agent was found to assist adhesive applications to the small fibers. The silane pretreatment included dipping the fiber tips in a 0.25% aqueous silane solution, followed by oven drying. This provided contin-

uous adhesive coverage rather than discrete adhesive droplet formation. Adhesive materials tested and found adequate included Devcon "5-minute" epoxy and Dow Corning 734 RTV self-leveling adhesive/sealant. The preferred adhesive material is the epoxy because curing occurs within an hour at room temperature. The RTV, in the quantities used, required a considerably longer curing time. The UV epoxy did not cure. Delivery reliability for glass fibers in the diameter range of 0.75 to 1.5 μm was approximately 90%.

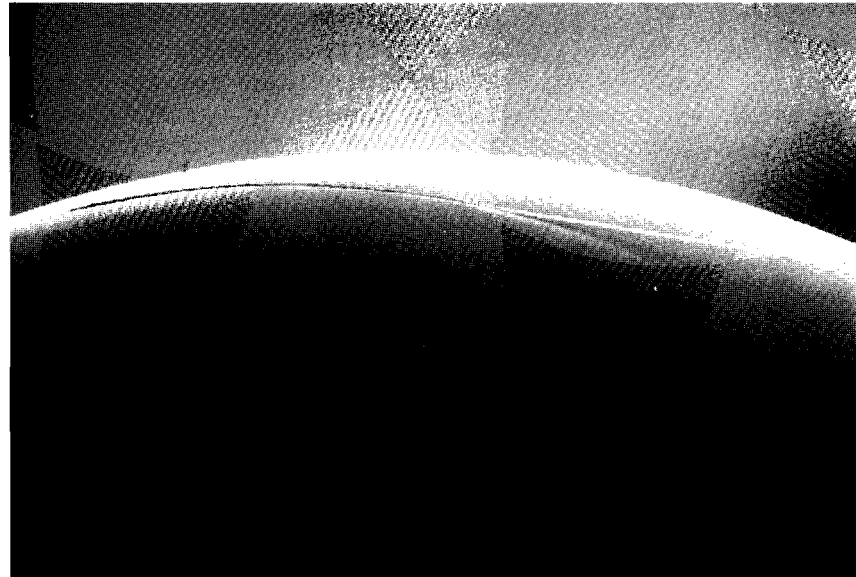
Fig. 30
Silk-fiber, target-mounting sequence. Single silk fibers are extracted (a), positioned in an assembly fixture (b), bonded to a fusion target (c), bonded to a drawn glass capillary (d), and shortened to the desired length (e).



Polymeric fiber, target-support material, in addition to having a density lower than that of glass, better matches the average atomic number of the outer ablative target surface. Because a commercial source of submicron polymeric fibers was not located, spider silk, a polymerized scleroprotein, was investigated with regard to its suitability for target delivery supports. One type of silk, viscid Ecribellatae web material,⁵ has been found to be extremely well suited for this application. The material is strong, is available in the diameter range of interest, and is coated with a natural adhesive. Two target-mounting procedures have been developed to reliably support fusion targets on submicrometer-diameter silk fibers for irradiation experiments.

The first assembly procedure produces a target that hangs vertically on a single 300- to 500- μm -long, 0.2- to 0.5- μm -diameter silk fiber. Assembly steps include positioning a silk strand on an assembly fixture, then attaching the target to one end and a drawn glass capillary to the other end. As illustrated in Fig. 30a, single silk strands are extracted with open tweezers from the edges of webs built in petri dishes containing a single Ecribellatae. The open tweezers are then positioned over a flat black aluminum assembly fixture, and the fiber is cut on both fixture sides with a razor to transfer the silk, as shown in Fig. 30b. A fusion target is positioned with a vacuum chuck into one of the 200- μm -deep vee grooves so that contact is made with the fiber (Fig. 30c). This step usually requires some fixture rotation under a side-illuminated stereo microscope to make the fiber visible. Silk material extending outside of the 3-mm separated parallel vee grooves is then cut. The point of a drawn glass capillary previously loaded into a magnetic target chamber positioner base is then contacted to the fiber in the second vee groove (Fig. 30d). Vertical motion of the horizontally oriented glass capillary causes separation of the fiber-mounted target from the assembly fixture (Fig. 30e). If initial fiber adhesion does not occur, repeated attempts usually produce bonding. The capillary is then rotated, causing fiber winding at the capillary tip, until the target-capillary separation distance is ~ 300 to 500 μm . The target-fiber adhesive contact is shown in the Fig. 31 SEM photograph. Precautions found necessary for successful completion of the procedure include shielding all described activities from air currents (including the operator's breathing), and maintaining a vertical target-capillary orientation after the fiber-shortening step is completed to prevent target-capillary attachment. Delivery reliability for single 0.25- to 0.5- μm -diameter silk was greater than 75%.

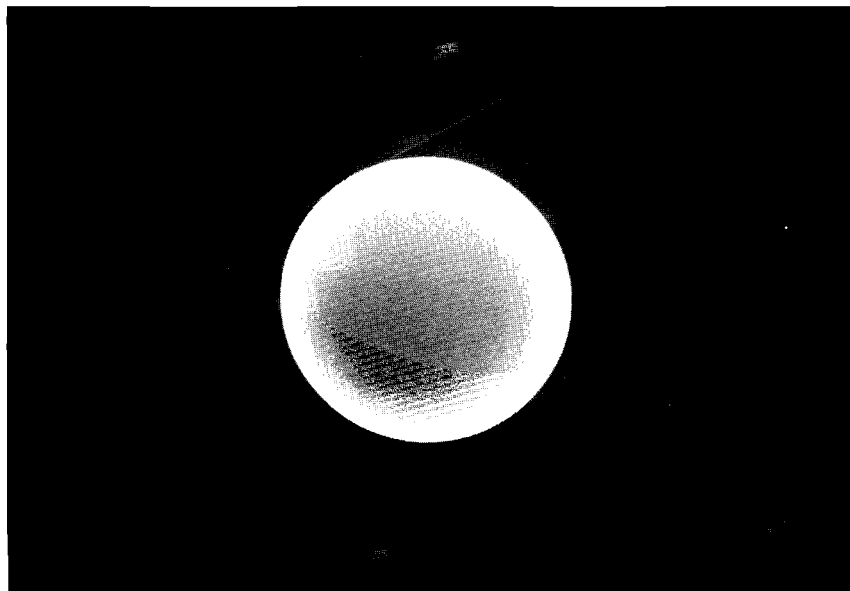
The second assembly procedure, a variation of the ring-mounting technique commonly used to support the fuel core in colliding shell targets, provides significant effective mass reduction over previously reported polymer films and fibers.^{6,7} Here, two fibers are positioned across a target-mounting ring or hemispherical shell. Excess silk material is then removed, and the target fuel core is placed between the separated fibers using a vacuum chuck. Figure 32 is an SEM photograph of a glass microballoon mounted in this configuration. Here the fiber diameters are approximately 0.4 μm , and the microballoon diameter is 400 μm . Solid steel ball bearings 500 μm in diameter have been reliably mounted and delivered with this procedure, an indication of the strength and surface adhesion of viscid Ecribellatae silk.



T494

10 μm

Fig. 31 SEM micrograph of fusion target showing viscous Ecribellatae silk adhesive contact area.



T518

400 μm

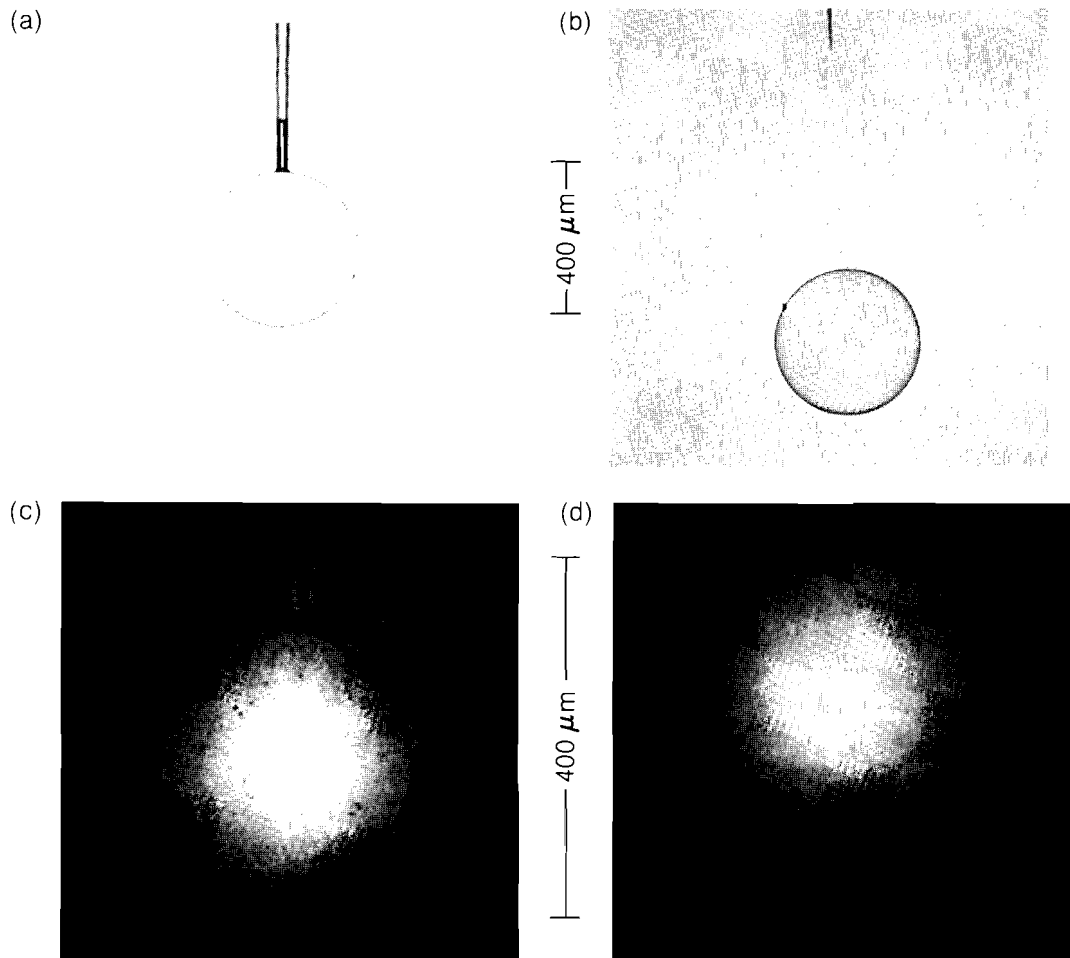
Fig. 32 Fusion target fuel core-mounted using two silk fibers in the geometry of a colliding shell target.

In both assembly procedures, no adhesive application was required for supporting targets using viscid *Ecribellatae* silk. The natural "sticky" silk surface was sufficient for reliable bonding.

Fig. 33
Comparison target micrographs and x-ray
implosion images.

- a) Conventional drawn glass capillary
mount
- b) Viscid *Ecribellatae* silk mount
- c) Soft x-ray pinhole image produced
by (a)
- d) Soft x-ray pinhole image produced
by (b)

Improved implosion symmetry has been demonstrated using the new support methods. Soft x-ray pinhole images produced by two comparison targets that were irradiated under similar conditions, along with target micrographs, are shown in Fig. 33.⁹ Figure 33a shows a target mounted using a conventional drawn glass capillary. The corresponding pinhole image (Fig. 33c), shows marked asymmetry near the stalk. The newly developed viscid silk mount (Fig. 33b) permitted a more symmetric implosion (Fig. 33d). No stalk perturbation is evident here. Similar improvements have been found using the submicrometer glass-fiber mounts.



T521

Minimum effective support mass was achieved using single 0.25- μm -diameter viscid Ecribellatae silk having an estimated density of 1.2 g/cm³. This material closely matches the average atomic number of target ablation layers and does not require adhesive application for target bonding, an important practical advantage. Drawn glass fibers with diameters $\geq 0.75 \mu\text{m}$ have been reproducibly fabricated and have been shown to reliably support targets for irradiation experiments. This type of fiber has a higher density (2.5 g/cm³) than the silk material and does require adhesive application. Commercial glass fibers, even though available down to 0.3 μm in diameter, presented practical difficulties that were not overcome for diameters less than 2 μm . Although target delivery will ultimately involve nonmechanical supports, the new mounting developments reported here are expected to postpone the need for conducting irradiation experiments with injected or levitated targets.

REFERENCES

1. The following papers describe various nonmechanical delivery approaches. Each approach would require considerable hardware development and refinement before implementation in our 24-laser-beam target chamber.
 - J. L. Pack, T. V. George, and A. G. Englehardt, *Rev. Sci. Instrum.* **39**, 1697 (1968).
 - D. B. VanHulsteyn and L. Anderson, *Rev. Sci. Instrum.* **44**, 453 (1973).
 - D. Burgeson, KMS Fusion, Inc., Annual Report (1978).
 - S. L. Milora, G. A. Foster, D. H. Edmonds, and G. L. Schmidt, *Phys. Rev. Lett.* **42**, 97 (1979).
2. B. Cranfill, E. H. Farnum, A. T. Lowe, and J. R. Miller, *Technical Digest of Topical Meeting on Inertial Confinement Fusion* (Optical Society of America, Washington, DC, 1978), Report ThE 2-1.
3. The source for this material was suggested by D. Steinman.
4. E. G. Diacumakos, "Methods for Micromanipulation of Human Somatic Cells in Culture," in *Methods in Cell Biology*, edited by David M. Prescott (Academic Press, New York, 1973), Chap. 15, pp. 290-296.
5. B. J. Kaston, *Natur. Hist.* **75**, 27 (1966).
6. Ye. G. Gamilii, A. I. Gromov, A. I. Isakov, L. A. Krupinina, Yu. S. Leonov, F. I. Matveeva, Yu. A. Merkul'ev, A. I. Nikienko, Ye. R. Rychkova, and G. V. Sklizkov, *Akademiia Nauk SSSR, Fizicheskii Institute Imeni P.N. Lebedev, Trudy* **94**, 29-60 (1977) (Translated-LA-TR-78-21).
7. *Inertial Fusion Program, Progress Report, 1 January-30 June 1978*, L-7587-PR, Los Alamos Scientific Laboratory (May 1980), pp. 146-147.
8. D. J. Borror, D. M. DeLong, and C. A. Triplehorn, *An Introduction to the Study of Insects* (Holt, Rinehart, Winston, 1976), pp. 94-121.
9. M. C. Richardson and D. M. Villeneuve, Laboratory for Laser Energetics, University of Rochester, unpublished data, 1982.